MACHINE INDUCED BACKGROUNDS IN THE FCC-ee MDI REGION AND BEAMSTRAHLUNG RADIATION

A. Ciarma*, E. Perez, G. Ganis, CERN, Geneve, Switzerland
M. Boscolo, INFN-LNF, Frascati, Italy

Abstract

The design of the Machine Detector Interface area (MDI) for the Future Circular Collider (FCC) is particularly challenging. Initial studies published in 2018 in the FCC Concept Design Report (CDR) are now being enhanced in the context of the ongoing FCC Feasibility Study. With respect to the CDR, a new design for the beam-pipe central chamber of the e+e- collider (FCC-ee), featuring a smaller radius and shorter length, is being considered. The new design allows for an inner layer of the Vertex Detector Barrel to be placed closer to the interaction point. The effect of the background induced occupancy due to Incoherent Pairs Creation (IPC), beam losses in the MDI area and Synchrotron Radiation have been investigated for the CLD detector, one of the detector concepts considered for FCC-ee. The characterisation of the intense Beamstrahlung radiation produced at FCC-ee is also presented.

INTRODUCTION

Machine induced background studies were performed for the FCC-ee Conceptual Design Report (CDR) [1], including the beam losses in the Interaction Region (IR), pairs production and the development of Synchrotron Radiation (SR) masks and shieldings. After the CDR, the design of the beam pipe central chamber has changed to a reduced radius of R=10 mm and length of L=18 cm (originally R=15 mm and length of L=25 cm), allowing to have the inner layer of the Vertex Detector Barrel closer to the Interacion Point (IP).

The Vertex Detector (VXD) geometry description of the CLIC-Like Detector concept (CLD) [3] has been modified in order to fit the new FCC-ee MDI region and to study the effects of several beam induced backgrounds. In particular, the first and the second layers of the barrel have been reduced both in radius to keep the same distance from the beam pipe, and in length in order to to preserve the angular acceptance of the original design. Also, the number of sectors in the innermost layer has been reduced from 16 to 12 because the staves' width is constrained by the manufacturing process. A sketch of the new version of the CLD VXD barrel is shown in Fig. 1. To the same purpose, a re-design of the IDEA [4] Vertex Detector is currently work in progress.

In addition to the design of the 10 mm radius central part of the beam pipe and consequent modifications to the detectors, also the design of the lattice has progressed since the CDR. The current instance of the collider has 4 IPs and different beam parameters. The parameters considered for the studies presented in this work are reported in Table 1.
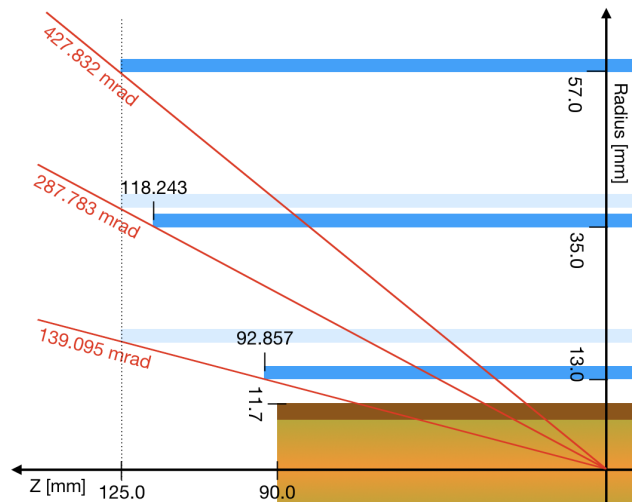
* Corresponding Author, andrea.ciarma@cern.ch

Figure 1: Sketch of the new design of the CLD VXD barrel. The blue shapes represent the dimensions of the layers in the new version, the light blue shapes refer to the CDR version. The gold shape is the beam pipe central chamber.

These modifications, together with the migration to the turnkey software Key4HEP [2], make it is necessary to repeat and extend the studies performed for the CDR. In this manuscript I present the status of the studies on the beam induced backgrounds due to the Incoherent Pairs Creation (IPC), beam losses due to failure scenarios, and synchrotron radiation on the CLD vertex detector and tracker. I also give the characterization of the beamstrahlung radiation produced at the IP at the four working points of FCC-ee.

INCOHERENT PAIRS CREATION

Secondary e^+e^- pairs can be produced via the interaction of the beamstrahlung photons with real or virtual photons

Table 1: FCC-ee beam parameters for the 4 IPs lattice

		Z	WW	ZH	t$\bar{\text{t}}$
GeV	E	45.6	80.0	120.0	182.5
nm rad	ϵ_x	71	2.16	64	1.49
pm rad	ϵ_y	1.42	4.32	1.29	2.98
mm	β_x/β_y	100/0.8	200/1	300/1	1000/1.6
μm	σ_x	8.426	20.78	13.86	38.60
nm	σ_y	33.70	65.73	35.92	69.05
mm	σ_z	15.4	8.01	6.0	2.8
10^{11}	N_e	2.43	2.91	2.04	2.37
1	N_{bunch}	10000	880	248	40

emitted by each particle of the beams during the bunch crossing. Some of the so produced particles will pass through the detector generating background. The occupancy O induced by a bunch crossing in a subdetector is defined as:

$$O = h \cdot A_{sensor} \cdot S_{cluster} \cdot S_f$$

where h is the hit density per bunch crossing in each subdetector, A_{sensor} is the surface area of the sensors, $S_{cluster}$ is the cluster size, and S_f is a safety factor. The VXD uses silicon pixels of $A_{sensor} = 25\,\mu m \times 25\,\mu m$, while the tracker (TRK) uses silicon strips of $1\,mm \times 0.05\,mm$. The cluster sizes considered for the VXD and the TRK are $S_{cluster}$=5 and $S_{cluster}$=2.5 respectively. For this study, a safety factor of $S_f = 3$ has been considered.

The generator used to produce the primaries for this study is GuineaPig++ [6], and the particles have been tracked in the CLD design using Key4HEP. Table 2 shows the number of pairs produced per bunch crossing and the maximum occupancy measured in each detector.

Table 2: Number of pairs produced per bunch crossing (BX) at the four working points, and maximum occupancy measured in the barrel and endcaps of the vertex detector and tracker (respectively VXDB, VXDE, TRKB, TRKE).

		Z	WW	ZH	t$\bar{t}$
1	Pairs/BX	1300	1800	2700	3300
10^{-6}	O_{max}(VXDB)	70	280	410	1150
10^{-6}	O_{max}(VXDE)	23	95	140	220
10^{-6}	O_{max}(TRKB)	9	20	38	40
10^{-6}	O_{max}(TRKE)	110	150	230	290

The induced occupancy increases with the beams energy. This is due to two factors: the pair production cross-section is enhanced [6], and due to the kinematics of the process more particles will enter the detector acceptance region as shown in Fig. 2.

The occupancies reported in Table 2 are all well below the percent, but depending on the electronics readout time the sensors may integrate signal over several bunch crossing. The estimate for the occupancy pile-up considering a bunch spacing Δt and readout window W_r can be obtained according to:

$$O(W_r) = O(BX)\frac{W_r}{\Delta t}$$

As shown in Table 3, even considering a readout window of W_r=10 μs - which is a conservative value - the maximum occupancy remains below the percent almost everywhere, except for the VXD barrel and TRK endcaps at the Z working point where it reaches values up to 2~3%. While the pileup of the detectors has not been defined yet, it will be important to overlay this background to physics events in order to verify the reconstruction efficiency as a function of the readout window.
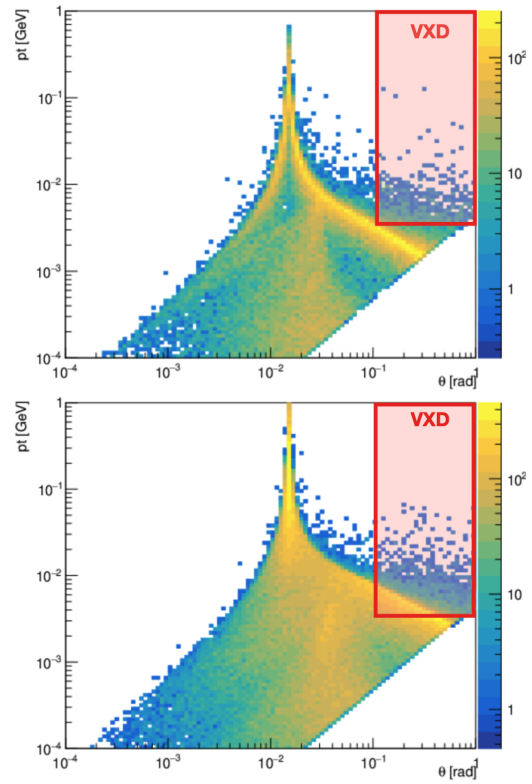
Figure 2: Production kinematics of the IPC at the Z (top) and $t\bar{t}$ (bottom) working points. The red area indicates the acceptance of the VXDB first layer.

BEAM LOSSES DUE TO FAILURE SCENARIOS

Several effects can lead to an increase of the beam emittance and consequent losses due to these particles impacting on the main collimator. This can be defined as a failure scenario. The deflected particles travel through the machine and a fraction will hit the beam pipe in the MDI region. The considered scenario is a drop of the beam lifetime down to 5 minutes due to halo losses on the primary collimator (located in point-F of the FCC-ee ring). The halo particles of a 182.5 GeV beam scattered by the primary collimator have been tracked for 700 turns in the latest lattice using X-Track [7], and the particles hitting the beam pipe in the ±7 m from the Interaction Point A have been tracked in the

Table 3: Average bunch spacing at the four working points, and maximum occupancy in the VXD and TRK considering a readout window (RW) of 1 μs and 10 μs.

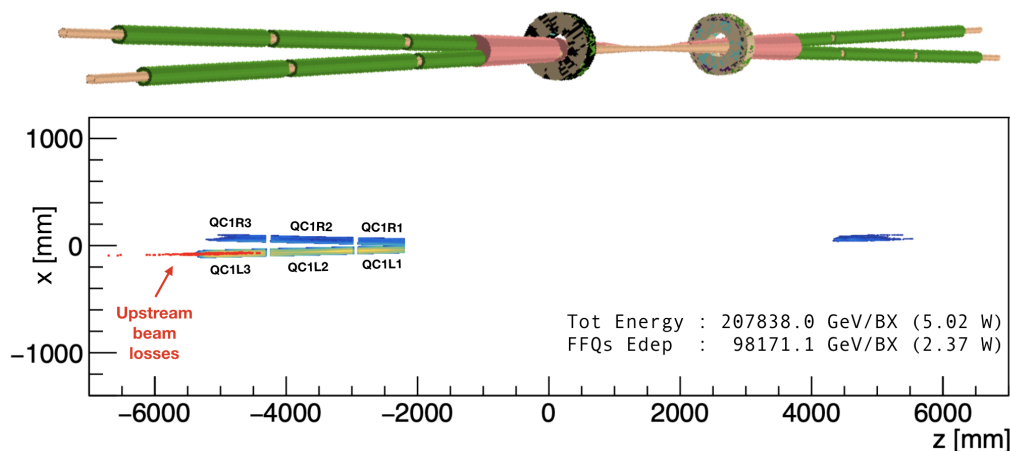|		Z	WW	ZH	t$\bar{t}$
ns	average bunch spacing	30	345	1225	7598
10^{-3}	O_{max}(VXD), RW=1 μs	2.33	0.81	0.05	0.18
10^{-3}	O_{max}(VXD), RW=10 μs	23.3	8.12	3.34	1.51
10^{-3}	O_{max}(TRK), RW=1 μs	3.66	0.43	0.12	0.13
10^{-3}	O_{max}(TRK), RW=10 μs	36.6	4.35	1.88	0.38

Figure 3: Top: FCCee MDI region model used in Key4HEP simulations, QC1 elements in green. Bottom: power deposited on the FFQs due to the considered failure scenario at IPA for $t\bar{t}$ energy.

CLD model of Key4HEP. The estimated loss rate in the IPA MDI area for this specific case is 1.5×10^8 Hz.

The primary beam losses are localised at 4~5 m from the IP, in correspondence of the magnetic elements of the innermost Final Focusing Quadrupole (FFQ) QC1. In order to study the deposited power on these magnets, simple cylindrical models composed of the equivalent material of the current design [8] have been introduced in the Key4HEP simulation as shown in the top of Fig. 3. The plot in the bottom part of Fig. 3 shows how the energy deposition in the FFQs due to the beam losses is mostly localised in the upstream elements (the closest to the losses) and accounts for about 2.5 W, which is about half of the total power carried by the losses. While the performance of the cryogenic system are yet to be defined, preliminary calculations show that this value should be below the quench limit of the superconductive quadrupoles. Dedicated studies on the power density deposition are currently in progress.

In terms of background, the induced occupancy in the CLD vertex detector and tracker is shown in Fig 4. The acronyms in the legends refer to: Vertex Detector barrel and endcaps (VXDB, VXDE), Inner and Outer Tracker barrel and endcaps (ITB, ITE, OTB, OTE). The particle from the beam hitting the beam pipe will produce a shower of secondaries, causing the occupancy to rise up to several percent points in particular in the IT. Please note that these plots refer to the occupancy due to a single beam, as it can be seen by the asymmetric distribution along the z-axis in the IT occupancy. Since the background level is higher than the rule-of-thumb value of 1%, further studies are needed to understand the impact on tracking efficiency and devise appropriate mitigation strategies.

SYNCHROTRON RADIATION MASK AND SHIELDINGS

The Synchrotron radiation produced by the last upstream dipole and by the final focusing quadrupoles can be a major source of background. In order to protect the detectors and mitigate the backgrounds, the use of a set of Tantalum masks internal to the beam pipe placed at the exit of the final focus quadrupole QC1 have been proposed in the CDR [1]. For the feasibility study the height of the mask has been increased from 5 mm to 8 mm in order to account for the reduced central chamber radius. Also, Tungsten shieldings have been designed to further minimise the number of photons which may scatter off the tip of the mask and produce showers in the detector.

A preliminary study has started to assess the efficiency of both masks and shieldings with the new lattice and IR. The shieldings in particular in their current design weight 180 kg per arm which should be supported by the beam pipe itself, so the possibility to reduce it while keeping sufficient protection for the detectors should be explored. Synchrotron radiation photons produced by the last downstream dipole at the $t\bar{t}$ working point have been generated using the Geant4 based toolkit BDSim [9], and have been tracked in the CLD model using Key4HEP. The energy distribution of the photons just before the Tantalum mask is shown in the left of Fig. 5. Due to the critical energy of O(100 keV) the interaction of these photons with the Tantalum mask is dominated by photoelectric effect, as shown in the right of Fig. 5.

From preliminary tracking, most of the secondaries produced by the photons impacting on the mask are efficiently absorbed by the mask itself. Anyway special attention should be given to the photons which interact with the very tip of the mask. The photoelectrons emitted near the surface of the mask can escape and reach the detector causing background. As a first approach, a monochromatic pointlike 1MeV photon beam has been simulated impinging 50 μm from the edge of the mask, and tracking in the CLD detector showed a large number of hits in particular in the tracker endcaps.

More detailed studies are currently in progress in order to understand better the impact of this potential source of background, and the effect of the Tungsten shieldings.
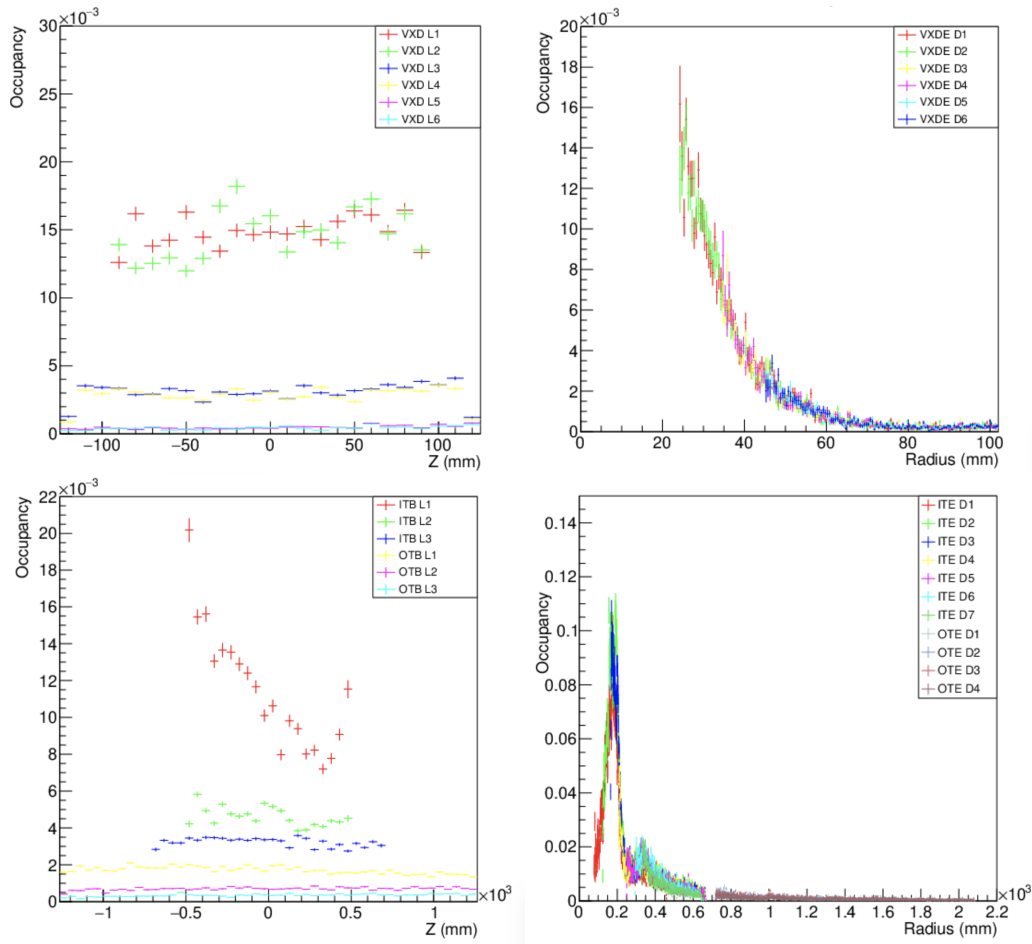
Figure 4: Occupancy induced by the beam losses in the VXD and IT/OT barrel layers (L) and endcap disks (D).
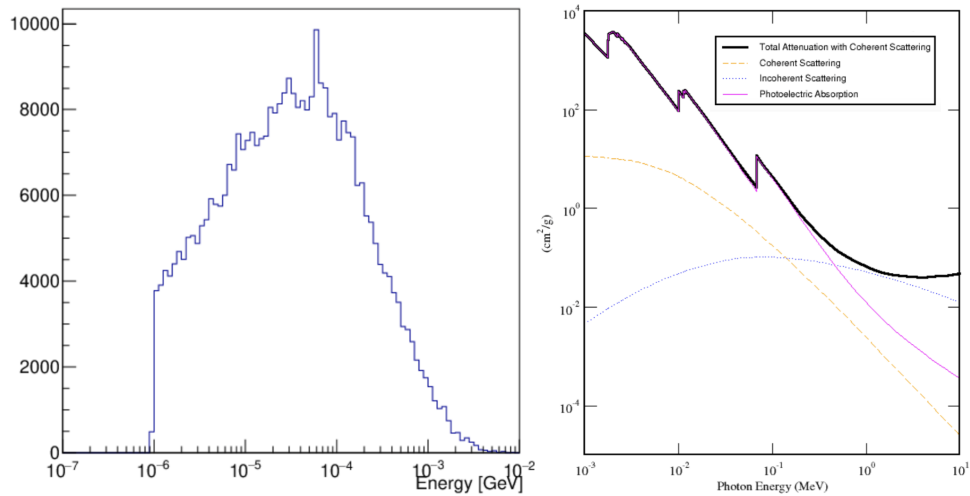

Figure 5: Left: energy spectrum of the SR photons just before the tantalum mask. Right: cross section for the interaction of photons with Tantalum [10].

BEAMSTRAHLUNG RADIATION CHARACTERIZATION

During bunch crossing each particle experiences the field generated by the charges of the opposing bunch and can be deflected, therefore emitting radiation in a similar way to Synchrotron Radiation. This process is called Beamstrahlung. The radiation is characterised by the dimensionless beamstrahlung parameter Υ [11], defined for gaussian beams as:

$$\Upsilon \sim \frac{5}{6} \frac{r_e^2 \gamma N_e}{\alpha \sigma_z (\sigma_x + \sigma_y)}$$

The beamstrahlung parameter depends on the beams energy E and population N_e, and on the bunch shape at collision σ_x, σ_y and σ_z. Due to the very small bunch size and high population, at FCC-ee the main driver for the bunch length and energy spread is beamstrahlung. At FCCee this parameter is in the region $\Upsilon \ll 1$, where the average number of photons emitted per particle n_γ, and their average energy $< E_\gamma >$ can be evaluated according to:

$$< E_\gamma > \sim E \times 0.462 \Upsilon$$

$$n_\gamma \sim 2.54 \left[\frac{\alpha^2 \sigma_z}{r_e \gamma} \Upsilon \right] \frac{1}{[1 + \Upsilon^{2/3}]^{1/2}}$$

The beamstrahlung radiation produced at FCC-ee has been simulated using the generator GuineaPig++. Due to the high bunch population and small beam size the radiation produced by each beam at the IP is extremely intense, up to several hundreds of kilowatts, as shown in Fig. 6.
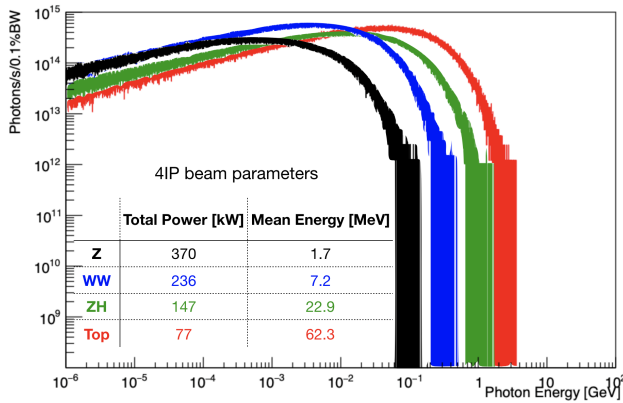

Figure 6: Energy spectrum of the beamstrahlung radiation produced at FCC-ee by each beam during bunch crossing for the four working points.

The photons are emitted collinear to the beam in a very narrow cone proportional to the inverse of their energy. As shown in Table 4, the dominant contribution to the photon beam divergence $\sigma_{px,py}^\gamma$ is the divergence of the lepton beam which produced it $\sigma_{px,py}^e$, resulting in values in the order of O(50∼100).

The photons will travel from the IP and hit the beam pipe at the first bending magnet. Tracking the photons in the GDML model of the downstream beam pipe show that the hits will be centred about 50 m from the IP, as shown in Fig 7 for the Z working point (similar scenarios apply for the other working points).

Due to the very high power carried by the radiation O(100 kW) it is necessary to have a beamstrahlung photon beam dump for each downstream side of each IP. The design of a dedicated photon extraction line leading to the dump needs to fulfil several constraints.
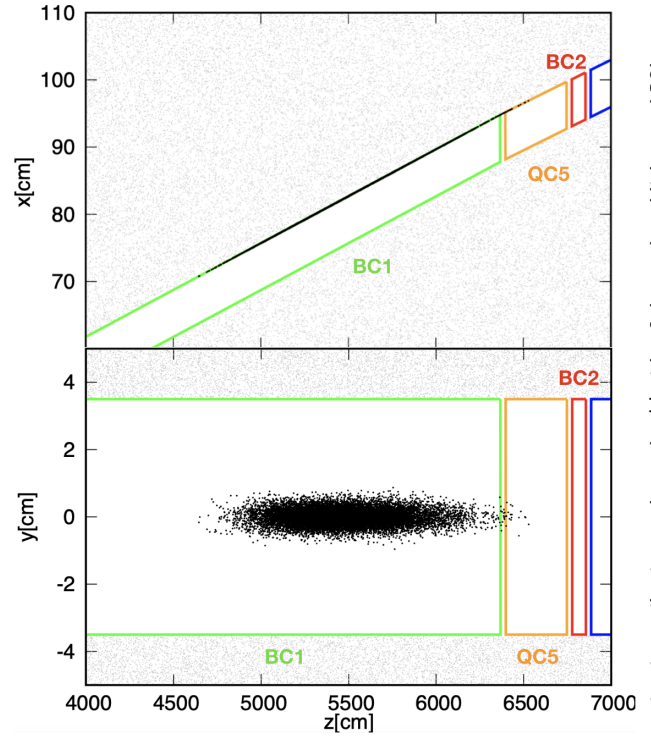

Figure 7: Location of the beamstrahlung photons hits on the beam pipe, for the Z working point.

First of all, while the transverse spot size of the photons at 50 m from the IP is well contained in a few cm^2 (see Table 4), because of the very low impinging angle the shadow of photons on the beam pipe wall is several meters long. Therefore the photon extraction window should be sufficiently large, as shown in the top of Fig. 8.

Also, in order to protect the beam pipe from secondary particles which could escape the beam dump, it is necessary to extend the extraction line to make space for sufficient shielding material. The bottom of Fig. 8 shows the separation between the lepton beam line and the beamstrahlung photon beam as a function of the distance from the IP. To obtain a separation of 1 m the beam dump should be placed at about 250 m from the IP. The integration of such line with the current design of the cavern (also with the possibility to have a dedicated tunnel) is currently under study.

Table 4: Divergence at the IP of the beamstrahlung radiation and the electron beam, photon spot size 50 m from the IP.

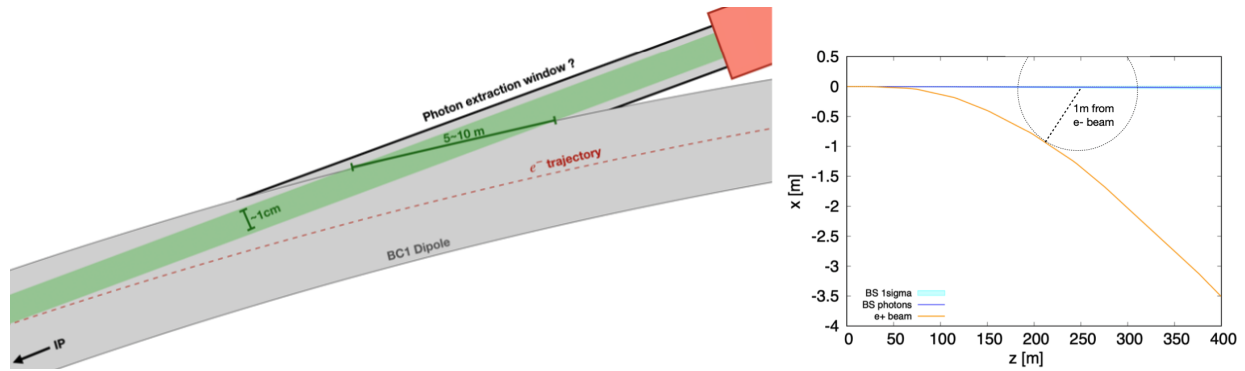|		Z	WW	ZH	tt̄
σ_{px}^γ	[μrad]	91.8	110.0	51.7	44.6
σ_{py}^γ	[μrad]	49.2	73.0	41.3	50.3
σ_{px}^e	[μrad]	84.3	103.4	46.2	38.6
σ_{py}^e	[μrad]	42.1	65.7	35.9	43.2
σ_x^γ @50 m	[mm]	4.59	5.50	2.58	2.23
σ_y^γ @50 m	[mm]	2.46	3.65	2.06	2.51

Figure 8: Left: sketch of the dedicated photon extraction line (not to scale). Right: separation between the beamstrahlung photons and the lepton beam.

CONCLUSIONS AND NEXT STEPS

The status of the beam induced background studies at FCC-ee, and the characterization of the beamstrahlung radiation produced at the IPs have been presented.

The occupancy in the CLD vertex detector due to the Incoherent Pairs Creation is below the 1% for all working points, also assuming conservative values for the sensors readout time.

The occupancy induced by a reduction of the beam lifetime down to 5 minutes at the $t\bar{t}$ energy can rise up to 10%. Further studies will cover the other working points, as well as different failure scenarios.

Preliminary studies on the Synchrotron Radiation induced background started. The absorption efficiency of the Tantalum mask on the radiation produced by the last upstream dipole at the $t\bar{t}$ working point showed that while most of the radiation is absorbed, the secondary electrons emitted near the tip of the mask can escape and generate background in the detector. Dedicated studies are currently going on to focus on this potential source of background and on the effect of the Tungsten shieldings.

The beamstrahlung radiation carries up to several hundreds of kilowatts, and hits the beam pipe at the first downstream dipole, an about 50 m from the IP. A dedicated photon extraction line and beam dump must be designed to deal with the extremely high power. The possibility to instrument the beam dump in order to measure properties of the colliding beams is also under investigation.

ACKNOWLEDGEMENTS

REFERENCES

[1] A. Abada *et al.*, "FCC-ee: The Lepton Collider", *Eur. Phys. J. Spec. Topics*, vol. 228, no. 2, pp. 261–623, 2019. doi:10.1140/epjst/e2019-900045-4

[2] G. Ganis, C. Helsen, and V. Völkl, "Key4hep, a framework for future HEP experiments and its use in FCC", *arXiv:2111.09874*. doi:10.48550/arXiv.2111.09874

[3] N. Bacchetta *et al.*, "CLD – A Detector Concept for the FCC-ee", *arXiv:1911.12230*. doi:10.48550/arXiv.1911.12230

[4] M. Antonello, "IDEA: A detector concept for future leptonic colliders", *Nuovo Cimento C*, vol. 43, p. 27, 2020. doi:10.1393/ncc/i2020-20027-2

[5] C. Rimbault, P. Bambade, K. Mönig, and D. Schulte, "Incoherent pair generation in a beam-beam interaction simulation", *Phys. Rev. Spec. Top. Accel Beams*, vol. 9, p. 034402. doi:10.1103/PhysRevSTAB.9.034402

[6] D. Schulte, Ph.D. thesis, University of Hamburg, *Report No. TESLA-97-08*, 1996.

[7] Online Available: https://xsuite.readthedocs.io/en/latest/

[8] M. Koratzinos, private communications.

[9] L. J. Nevay *et al.*, "BDSIM: An accelerator tracking code with particle–matter interactions", *Comput. Phys. Commun.*, vol. 252, p. 107200, 2020. doi:10.1016/j.cpc.2020.107200

[10] M. J. Berger *et al.*, "XCOM: Photon Cross Section Database (version 1.5)". Online Available: http://physics.nist.gov/xcom. National Institute of Standards and Technology, Gaithersburg, MD., 2010. doi:10.18434/T48G6X

[11] K. Yokoya, P. Chen, "Beam-Beam Phenomena in Linear Colliders", *Lect. Notes Phys.*, vol. 400, pp. 415-445, 1996 (and online 2005). doi:10.1007/3-540-55250-2_37